

An Examination of Forwarding Prediction Metrics in Dynamic Wireless Networks

Joseph P. Macker, Jeffery W. Weston

Information Technology Division, Naval Research Laboratory, Washington DC

Email: joseph.macker@nrl.navy.mil, jeffery.weston@nrl.navy.mil

Abstract—This work studies centrality metrics as forwarding load predictors, for both unicast and multicast traffic, within dynamic ad hoc network topologies. We present results from a series of emulation experiments based around an emergency response mobile network scenario. From collected temporal topological and traffic data, we calculate a rank correlation measure between predictive centrality metrics and actual observed traffic forwarding by nodes using several mobile topologies. We include the examination of a localized bridging centrality metric, previously developed, along with several well-known centrality measures. We show that under static conditions, all predictive metrics are extremely accurate; whereas under different motion conditions, there are reduced levels of accuracy. Yet, even during mobility cases, the ranking correlation between measured forwarding and the predictive metrics stays moderately positive throughout the experiments. We demonstrate stronger overall correlation in the unicast traffic flow cases and our localized bridging centrality tracks well in accuracy with other global state centrality metric variations. As expected, multicast forwarding scenarios are more challenging and show somewhat lower correlation in overall ranking prediction. Perhaps surprisingly, localized bridging centrality frequently outperforms other centrality metrics in mixed mobility cases for the multicast routing flows examined. Much of this work is preliminary and we discuss ongoing challenges, potential applications, and further planned work. Early results regarding the use of localized bridging centrality as a predictive measure for traffic forwarding are encouraging.

I. INTRODUCTION

The technical objective of this work is to apply complex network analytics as an aid in traffic load prediction and management of dynamic routing mobile ad hoc network (MANET) systems. Such a capability, if effective, will provide improved analytics for dynamic wireless networks that can aid both mission planning and real-time management of such systems. Since the goal is to provide dynamic prediction estimations of relative traffic forwarding and loading, the techniques can also inform related cyber systems, such as helping to determine key network nodes or links in an evolving routing structure. In addition, analytic feedback can also be used to further defend or optimize a local routing neighborhood in a distributed system. The application is not limited to MANET systems, but we will focus on specific MANET-type dynamic routing such as connected dominated set (CDS) based multicast forwarding.

While there are many potential approaches to structural analytics, here we focus on examining a variety of centrality measures [1], [2] and apply the resulting coefficients to predict relative rankings of a network node's likelihood to perform traffic forwarding within a particular mobile topology.

Centralities generally represent the statistical ranking of the importance or influence of vertices (i.e., nodes) or edges within a network graph, based upon a particular structural or interaction model. Many centrality measures have strong relationships to statistical mechanics models and are therefore often useful in predicting forms of behavior or dynamic performance of topological node interaction. This paper focuses in particular on applying centrality concepts to predict the relative importance of certain nodes and links as traffic forwarders within a MANET.

Different forms of MANETs exist and they often have differing concepts of forwarding behavior that may include multipath or mesh forwarding behaviors. Multiple routing protocols may also run simultaneously within a network and serve different types of network traffic (e.g., unicast vs. multicast routing). As an example, betweenness centrality and shortest cost path unicast routing classes are closely aligned conceptually, so we expect this centrality to be a good predictor of shortest path routing behavior. However, the dynamic mesh forwarding nature of multicast and some other multi-path or adaptive mesh routing protocols are perhaps better served by alternative flow-based centrality models. The bridging centrality we will examine includes both shortest path and relative density properties to better identify nodes that serve as structural bridges important across a class of forwarding strategies for both unicast and multicast. Additional congestion, loss, and link dynamics within a network can actually cause the network protocol to redirect traffic even without mobility; therefore, we are interested in examining a variety of centrality measures and combinations of routing protocol classes within more realistic wireless system scenario models.

The bridging centrality metric we will examine is also a localized variant that may help reduce control communication, convergence time, and computation complexity. Centralities requiring the collection of global topology information are prohibitive in environments that include temporal disconnections of clusters, mobility, and/or bandwidth limitations. The localized 2-hop bridging centrality estimator was developed by the author in previous work [3]. Past related work showed potential benefits of localized bridging centrality to better manage MANET protocols, such as the dynamic MANET routing enhancements demonstrated in [4].

Another contribution of the work, beyond the use of a localized centrality to predict loading, is that we examine

performance in a non-uniform, mobile emulation model of a wireless emergency response network. While we do not examine the specific management, optimization, and cyber applications in this paper, we feel the proposed work has broad transition potential as a means to help classify, plan, design, and validate mobile networks intended to structurally operate while undergoing disruptive conditions. Motivation for this work is stimulated by ongoing proliferation of lower-cost heterogeneous wireless technology, autonomous mobile systems, and embedded computing devices resulting in novel opportunities for networking in disrupted battlespace operations. Distributed collaboration systems are also of interest within commercial and civil applications for safety, disaster relief, distributed sensor, robotics, and community networking applications.

The paper is organized as follows: In Section II, we introduce and review the centrality metrics used in the experimentation. Then in Section III, the routing approach is briefly described, followed by Section IV discussing the emulation modeling components used for experimentation. In Section V, we present temporal analytics of the various motion scenarios in terms of global invariant metrics, such as algebraic connectivity and density coefficients. Section VI presents and discusses the rank correlation results across several unicast and multicast test cases. Section VII discusses future work and we conclude in Section VIII with a summary discussion.

II. CENTRALITIES AND STATISTICAL TRAFFIC FLOW MODELS

For the purpose of centrality-based structural analysis and prediction, we model our mobile dynamic networks as a time series of weighted graphs represented as $G = (V, E, w, t)$, where V is the set of vertices (representing the data or nodes in the network) and E is the set of edges connecting the vertices in V . w represents a set of edge weights in E that may be asymmetric. In our examples, w represents a stochastic probability of packet reception given a wireless link quality and mobility model. As was demonstrated in [5], dynamic w values can be extracted from routing link quality metrics, such as expected transmission count (ETX) variants. t represents the time of the topological snapshot in a time-ordered graph sequence.

A. Variants of Flow-based Centrality Models

While there are a wide variety of centrality measures that have been developed to study complex network structures and behavioral relationships, we concentrate on a few flow-based centrality models. Variations of betweenness are one such class of centralities and several types and definitions are well covered in [6] and we have also considered variations of current flow models discussed in [7].

B. Betweenness and Load

The basic Betweenness Centrality is defined in Equation 1.

$$C_{bet}(v) = \sum_{s \neq v \neq t} \frac{\sigma_{st}(v)}{\sigma_{st}} \quad (1)$$

In Equation 1, σ_{st} is the total number of shortest paths from node s to node t and $\sigma_{st}(v)$ is the number of those shortest paths that pass through v . Betweenness centrality is a popular complex network measure and as mentioned in the introduction, its flow model assumptions are similar to many link-state based unicast protocols that calculate shortest path routes. One such protocol is the MANET Internet Standard Optimized Link State Routing (OLSR) protocol [8], [9]. In this work, we also examine *load* centrality, a close relative to betweenness centrality. The differences between betweenness and load centrality are summarized in [6]. Load centrality fundamentally differs from betweenness centrality by introducing a hypothetical flow model that splits commodity traffic equally among minimum geodesic distance paths towards the destination node. We also examined communicability betweenness [2] in our experiments, a metric which includes a model of all walks in the network, but overall the results generally showed lower correlation ranking than other centralities and we did not include these summaries.

C. Localized Bridging Centrality

Localized Bridging Centrality (LBC) was first presented in [10] and a localized k-hop variation (LBC-k) with weighted graphs was provided and studied in [5] for the 2-hop case. The 2-hop neighborhood variant is of direct interest in our study of MANET type routing, as 2-hop local graph information is often gathered and maintained by each node within a MANET routing domain as part of normal neighborhood discovery signaling. Equation 2 shows the formulation of LBC-k from [5]. The first term is altered from the global centrality definition and it converts a global betweenness centrality calculation to one that is localized within the k-hop ego network [11] of the node. The second term measures the relative density between a node's neighborhood and its neighbor's neighborhoods. We refer the reader to [5] for additional details and related studies.

$$LBC_k(v) = \sum_{s \neq v \neq t}^{s, t \in N_k(v)} \frac{\sigma_{st}(v)}{\sigma_{st}} * \frac{\frac{1}{d(v)}}{\sum_{i \in N(v)} \frac{1}{d(i)}} \quad (2)$$

III. ROUTING MODELS USED

As mentioned in Section I, centrality measures often represent statistical models of information flow, similar to how routing protocols may be designed with different forwarding models. In this study, we limit analysis to two different forms of MANET routing and traffic patterns. For unicast routing tests, we use a working prototype of the OLSRv2 protocol [9] as a variant of shortest cost link state routing. This implementation supports the use of dynamic link costs such as the Expected Transmission Count (ETX). To support multicast routing tests, we use a working prototype of the Simplified Multicast Forwarding (SMF) protocol [12] with a connected dominating set (CDS)-based forwarding relay set that is dynamically elected using the Essential Connected Dominating Set (ECDS) protocol specified in the Appendix of [12]. Localized 2-hop election information is gathered

using a version of the Neighborhood Discovery Protocol (NHDP) [13].

IV. EMULATION MODELING APPROACH

To examine a number of different mobility conditions and different traffic flow distributions, we extend a 21-node emergency disaster response scenario developed at the Naval Research Laboratory (NRL) as a fictitious, mission-oriented wireless ad hoc network deployment. We orchestrate this scenario using virtual network emulation components including the Common Open Research Emulator (CORE), the Network Mobility Framework (NMF), and the Extendable Mobile Ad hoc Network Emulator (EMANE) [14]–[16]. The scenario involves both pre-planned motion and causal event-driven motion elements. The non-causal motion pattern involves the looping of patrol vehicles orbiting a critical inner area perimeter road. For the static case, these nodes are kept at their initially distributed locations. We also include experiments that orchestrate motion causally induced by the exchange of network communication messages. An example is received orders causing repair teams, helicopters, or medical rescue teams to move to particular destination locations to perform further tasking. A snapshot of the scenario topology and node names are shown in Figure 1.



Fig. 1: Emergency Response Scenario

A. Measuring Rank Correlation

For each network experiment, our goal is to measure the ranking correlation between two data sets: traffic forwarding load amongst network nodes in time and some predictive centrality metric for a given temporal topology estimate. To do this, we require two data sets: mobile network topology estimates and traffic forwarding measures in time. Topologies are estimated within a given time interval (10 seconds) given relative node position and communication link quality and are extracted as a time series from the EMANE mobile network emulation system. For our 30 minute emergency response scenarios, we therefore have approximately 180 temporal graphs for each trial. These topology sequences provide the basis for the analytic baseline in calculating predictive metrics. For the LBC-2, only local 2-hop neighborhood information is used for each node’s calculation, therefore simulating limited state using information from a localized signaling protocol like NHDP [13].

B. Traffic Generation

The Multigenerator (MGEN) traffic tool [17] is used to load the network scenario with unicast and multicast traffic flows respectively. To provide a baseline traffic load for prediction, a set of all-to-all unicast and multicast network traffic flows are established so that each node in the test is both a source and sink of each traffic type. One packet per second is sent on each flow type from each source where a unicast packet is 512 bytes and a multicast packet is 100 bytes. Other mixed traffic flows were added to the experiment as well, but only limited testing of this nature was performed. Throughout the experiment, standard *packet capture* (pcap) and MGEN logs were collected. Individual node network forwarding data was extracted from a set of distributed pcap logs and summarized within a time window for the unicast and multicast routing experiments performed.

V. ANALYSIS OF MOTION SCENARIOS

Prior to examining rank correlation results, we here analyze a set of global invariant metrics on the topologies collected for the different motion scenario cases. In each plot, we show the time-varying values for the Fiedler value and a density coefficient on a 10 sec window of topology snapshots. The Fiedler value, also known as the algebraic connectivity, of a graph is the second-smallest eigenvalue of the Laplacian matrix of that graph. Its magnitude has been shown to reflect how well-connected an overall graph is. If the topology is disconnected in any manner, this value equals zero. The density coefficient is another indicator of average connectedness throughout the graph and we plot this as well.

Looking at the static motion case in Figure 2A, we see that all coefficients are stable throughout the scenario as they should be. The Fiedler value indicates the network is connected, but perhaps weakly. The density coefficient is also relatively low in value indicating the initial condition of the network may be somewhat sparse.

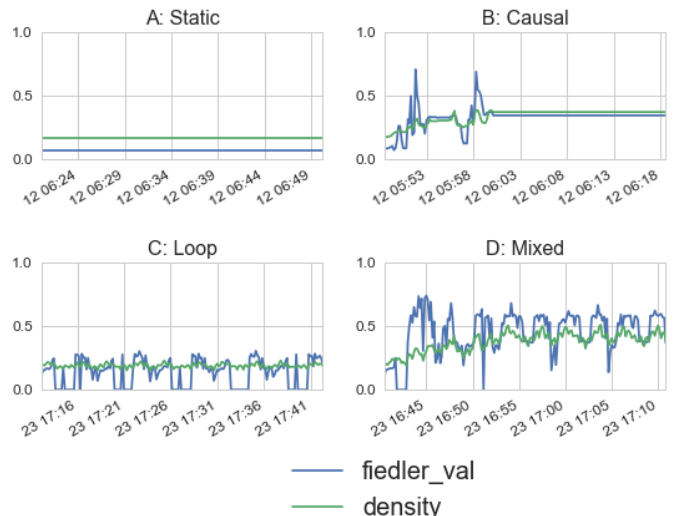


Fig. 2: Global Topology Metrics for Motion Cases

From the causal motion case in Figure 2B, we see that the coefficients begin at values consistent with the static case and that the Fiedler value and density coefficient increase in the first half of the scenario and then settle out to fairly stable values once causal nodes complete movement to event-driven locations. While fluctuating in topological strength in the beginning, the network settles out in a more strongly connected condition in the second half of this scenario since the causal nodes move to more central topological locations. In Figure 2C, we see a more interesting case of looping motion only, which has significant temporal strengthening and weakening of the topological structure. The Fiedler value shows periodic events in which the topology is temporarily disconnected and then reconnected as nodes proceed around the looping pattern. The overall density coefficient stays roughly consistent for the connected components during these periods. In Figure 2D, we see the mixed effect of looping motion and causal motion together. In this case, we see connected but periodically fluctuating conditions due to the combined effects of causal nodes and looping nodes within the topology.

As the Fiedler value may be a good single value indicator of strengthening and weakening of graph connectivity, we present a violin plot in Figure 3 which summarizes the temporal density distributions of coefficient values for each experimental case. We can see clearly that each case, except static, has temporal variability in values and that the looping motion case has more topological degradation and periodic disconnection events, shown by the broader distribution of lower Fiedler values. While it is not the main purpose of this paper, such analytic representations of complex dynamic topological scenarios may help better categorize non-parametric scenarios and further aid in interpreting complex network results in future work.

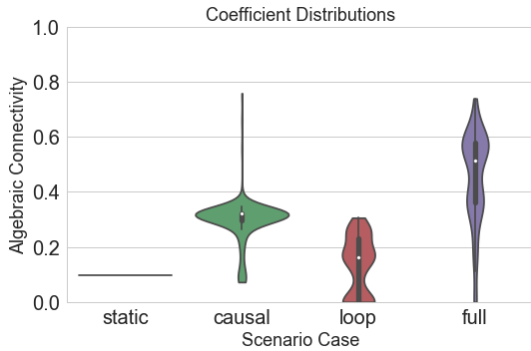


Fig. 3: Algebraic Connectivity Distributions

VI. ROUTING TESTS AND FORWARDING LOAD RANK CORRELATIONS

In this section, we briefly present a series of experiments for both unicast and multicast routing cases and discuss summary results using collected temporal rank correlation data. The title of each graph in this Section indicates the motion case of the scenario as previously discussed in Section V. The term A2A indicates all-to-all traffic flow was measured to perform the rank correlation. In each graph, we plot the Spearman rank

correlation scores [18] of three centrality values (betweenness, load, and local bridging (LBC-2)) in comparison to the relative traffic forwarding loads measured. In the Spearman correlation graphs to follow, we only plot the positive range [0,1] even though the Spearman coefficient range is [-1,1], as we observed only positive correlation scores in the cases presented.

A. Unicast Forwarding Tests

This section briefly presents a series of unicast traffic and routing tests and observations. Figure 4 shows the static motion case and it is somewhat trivial that load and betweenness centralities correlate well with observed OLSRV2 forwarder rankings within the network. What is perhaps more surprising is that LBC-2 also has a strong rank correlation value of around 0.9 throughout most of the test.

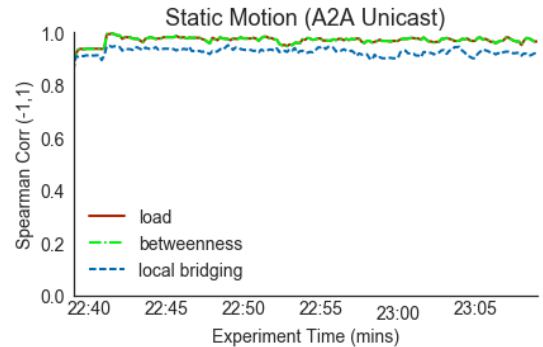


Fig. 4: Unicast Static Experiment

In Figure 5, we observe the causal motion case and we see that the relative load and betweenness centralities have fluctuating periods of correlation during the first 10 minutes of the experiment. Again, LBC-2 performs slightly poorer at times, but tracks well with the correlations of the other two metrics. Throughout the whole experiment, the results stay positively correlated and relatively high.

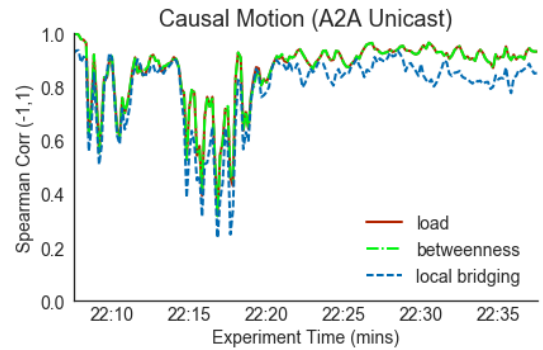


Fig. 5: Unicast Causal Motion Experiment

In Figure 6, we show the looping motion case and observe that load and betweenness centralities have fluctuating periods of correlation, but the correlation with forwarder ranking remains strong throughout the testing, generally much higher than during causal motion testing. Again, LBC-2 performs slightly poorer at times, but tracks well with the overall

dynamic correlations of the other two metrics and also remains in a strong correlation region for all looping motion. Again, throughout the experiment the results stay positive and relatively high. This is interesting to note, as we know from the algebraic connectivity that these topologies go through periods of disconnectivity which could have caused significant inaccuracy between the estimators and the dynamic MANET routing protocol.

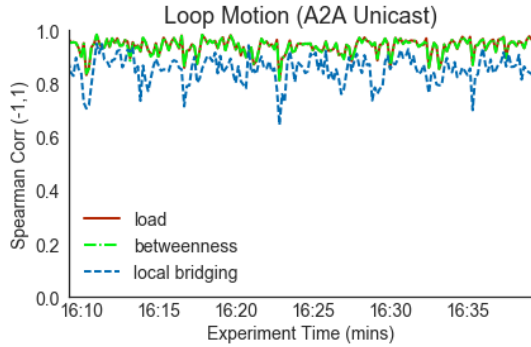


Fig. 6: Unicast Loop Motion Experiment

In Figure 7, we show the mixed case of looping and causal motion and we see that relative load and betweenness centralities along with the local bridging centrality have stronger fluctuating periods between strong and moderate correlation. These fluctuations continue to occur after the causal motion has stabilized. As seen from the motion analytics in Section V, the network reaches a higher density but the algebraic connectivity and the density coefficients continue to periodically fluctuate. This may possibly be explained by the fact that there are more opportunities for route changes once causal nodes have moved to more central locations within the network topology. Throughout the whole experiment the results stay positive, but they do now fluctuate between moderate and strong correlation coefficients. Again, local bridging centrality tracks well with the global centrality predictors and remains a viable alternative for predictive application with good correlation results.

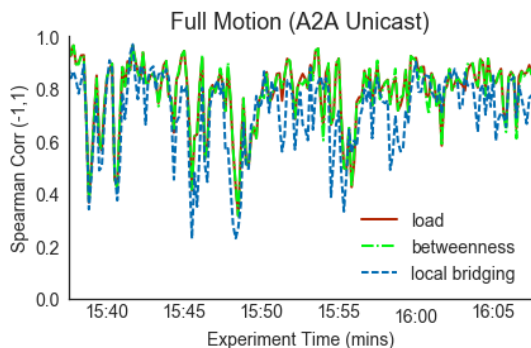


Fig. 7: Unicast Mixed Motion Experiment

B. Multicast Forwarding Tests

This section briefly presents a series of multicast traffic and routing test results and observations. In these cases, SMF with a self-organizing ECDS relay set was used as the multicast routing mechanisms within all networks under

test (with classical flooding, all nodes forward every packet so centralities are uncorrelated with forwarding statistics). Figure 8 shows the static motion case, and we now observe that centralities presented are only moderately correlated with actual forwarding statistics and fluctuate roughly between 0.3 and 0.6 through the testing. We should point out that the routing flow model has now moved away from a shortest path model to a multipath mesh forwarding model and we do expect less correlation. ECDS does provide some routing structure but it is not necessarily a shortest path structure.

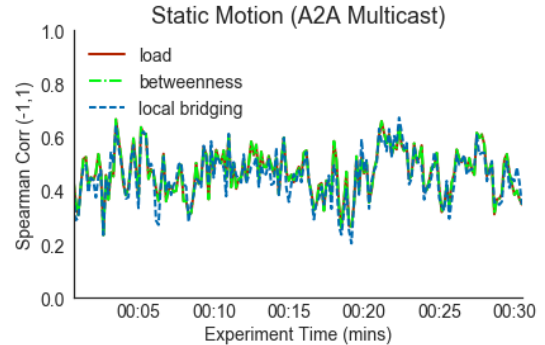


Fig. 8: Multicast Static Experiment

For the multicast case, Figure 9 now shows higher correlation for periods and improves in general over the static case. The increasing density caused by causal motion may provide a benefit in terms of multicast forwarding prediction correlation. Perhaps surprisingly, we now see at times the local bridging centrality is more strongly correlated than the global centralities. This may be simply due to the fact that the bridging statistical model has an element of density coverage similar to ECDS election heuristics. With looping motion, Figure 10 shows slightly poorer performance in general for local bridging but higher overall performance again versus the static case. Again, this may be due to the density increases after the initial phases of the motion scenarios. In the multicast forwarding case for mixed motion, Figure 11 shows some interesting results for local bridging centrality in that it seems to outperform other global centralities and has periods of relatively high correlation (0.6-0.9) vs. other mobility scenarios. This demonstrates perhaps some benefit in moving beyond purely shortest geodesic path metrics in more complex communication networks.

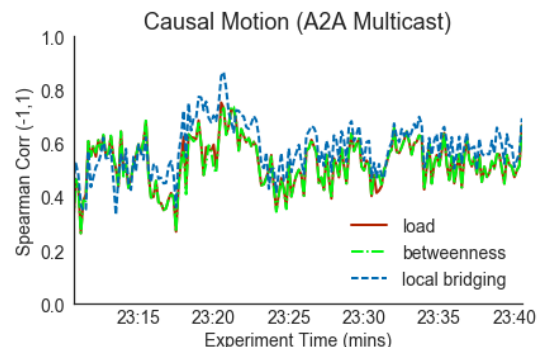


Fig. 9: Multicast Causal Motion Experiment

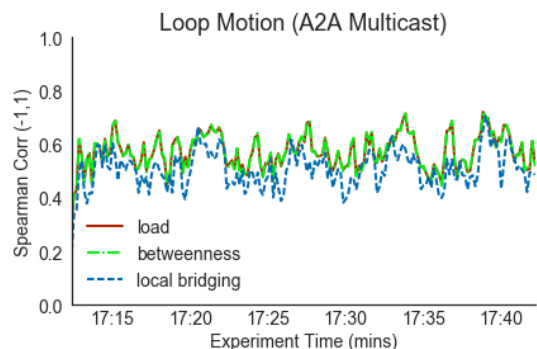


Fig. 10: Multicast Loop Motion Experiment

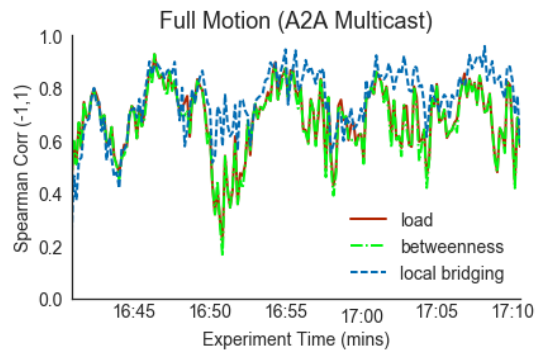


Fig. 11: Multicast Mixed Motion Experiment

VII. FUTURE WORK AND CHALLENGES

Centrality metrics which consider all nodes as balanced traffic sources/receivers have limitations. At present, centrality extensions exist for network subset computations, where certain sources and destinations can be provided to adjust the centrality flow model. This is applicable when portions of network nodes may serve primarily as network relays and not as active traffic sources and receivers. However, we are not presently aware of centrality work that addresses unbalanced flow models, so we see this as a future challenge to address this gap. An imagined approach is to combine work on predictive mission workflows at the communication level with the commodity exchange models underlying a centrality calculation, resulting in a cross-layer, mission traffic aware model. This could be adjusted during mission phases or transitions.

Significant levels of congestion and contention likely reduce the correlation resulting from simplistic centrality predictions. In these tests, we did use an underlying wireless model that included contention effects, but we did not directly measure the levels of contention. More work is planned to focus on contention and congestion conditions. Finally, we presented work with relatively small scenarios and plan to do work with larger scale systems and scenarios. However, the scale we tested at may be appropriate for many collaborative, tactical subnetwork deployments.

VIII. SUMMARY AND CONCLUSIONS

We presented a series of emulation results examining the ranking correlation between a set of complex network centrality coefficients and actual measured dynamic network forwarding load within a MANET. We included four motion cases

and modeled an emergency response wireless network scenario including unicast and multicast routed traffic. We examined a number of interesting effects by performing dynamic correlation metric studies comparing a class of centrality metrics to measured network forwarding load across the temporal network topologies in each case. We showed that as motion increases, the ranking correlation between the relative loading and centrality metrics stays moderately positive. We also demonstrated that LBC-2, a localized bridging centrality, does surprisingly well in predicting forwarding load as compared to a set of globally computed centrality metrics. In the multicast case, with mixed motion models, it was shown that LBC-2 often outperformed the other global centrality correlations as a rank predictor of network forwarders. This is encouraging and while the work is preliminary, effective prediction aids can improve distributed management, network cyber tactics, and localized optimization within such networks.

REFERENCES

- [1] Mark EJ Newman. The Structure and Function of Complex Networks. *SIAM Review*, 45(2):167–256, 2003.
- [2] Ernesto Estrada. *The Structure of Complex Networks: Theory and Applications*. Oxford University Press, 2011.
- [3] Joseph P Macker and Ian J Taylor. Prediction and planning of distributed task management using network centrality. In *Military Communications Conference (MILCOM), 2014 IEEE*, pages 859–864. IEEE, 2014.
- [4] Soumendra Nanda and David Kotz. Social Network Analysis Plugin (SNAP) for Mesh Networks. In *Wireless Communications and Networking Conference (WCNC), 2011 IEEE*, pages 725–730. IEEE, 2011.
- [5] J. P. Macker. An Improved Local Bridging Centrality Model for Distributed Network Analytics. In *2016 IEEE Military Communications Conference (MILCOM) Conference*, pages 600–605. IEEE, Nov 2016.
- [6] Ulrik Brandes. On Variants of Shortest-path Betweenness Centrality and their Generic Computation. *Social Networks*, 30(2):136 – 145, 2008.
- [7] Ulrik Brandes and Daniel Fleischer. *Centrality Measures Based on Current Flow*, pages 533–544. Springer Berlin Heidelberg, Berlin, Heidelberg, 2005.
- [8] T. Clausen and P. Jacquet. Optimized Link State Routing Protocol (OLSR), RFC 3626. IETF, October 2003.
- [9] T. Clausen and et al. Optimized Link State Routing Protocol (OLSR) version 2, RFC 7181. IETF, April 2014.
- [10] Soumendra Nanda and David Kotz. Localized Bridging Centrality for Distributed Network Analysis. In *Computer Communications and Networks, 2008. ICCCN'08.*, pages 1–6. IEEE, 2008.
- [11] Stephen P Borgatti, Ajay Mehra, Daniel J Brass, and Giuseppe Labianca. Network Analysis in the Social Sciences. *Science*, 323(5916):892–895, 2009.
- [12] J.P. Macker. Simplified Multicast Forwarding, (RFC 6621). *Internet Engineering Task Force (IETF) Experimental Internet Standard*, 2012.
- [13] T. Clausen, C. Dearlove, and J. Dean. Mobile Ad Hoc Network (MANET) Neighborhood Discovery Protocol (NHDP), RFC 7181. IETF, April 2011.
- [14] Jeff Ahrenholz, Claudiu Danilov, Thomas R. Henderson, and Jae H. Kim. CORE: A real-time network emulator. In *IEEE Military Communications Conference*, pages 1–7, 2008.
- [15] Natalie Ivanic, Brian Rivera, and Brian Adamson. Mobile Ad hoc Network Emulation Environment. In *Military Communications Conference, 2009. MILCOM 2009. IEEE*, pages 1–6. IEEE, 2009.
- [16] Jeff Ahrenholz, Tom Goff, and Brian Adamson. Integration of the CORE and EMANE Network Emulators. In *IEEE Military Communications Conference (MILCOM) Conference*, pages 1870–1875. IEEE, 2011.
- [17] Brian Adamson. The Multi-Generator (MGEN) User's and Reference Guide 5.0. <https://downloads.pf.itd.nrl.navy.mil/docs/mgen/mgen.html>, March 2017.
- [18] Charles Spearman. The Proof and Measurement of Association between Two Things. *The American Journal of Psychology*, 100(3/4):441–471, 1987.